

# Region-Wise Correspondence Prediction between Manga Line Art Images

Yingxuan Li<sup>1\*</sup>, Jiafeng Mao<sup>2</sup>, Qianru Qiu<sup>2†</sup>, Yusuke Matsui<sup>1</sup>

<sup>1</sup>The University of Tokyo, <sup>2</sup>CyberAgent, Inc.

## Abstract

Understanding region-wise correspondence between manga line art images is a fundamental task in manga processing, enabling downstream applications such as automatic line art colorization and in-between frame generation. However, this task remains largely unexplored, especially in realistic scenarios without pre-existing segmentation or annotations. In this paper, we introduce a novel and practical task: *predicting region-wise correspondence between raw manga line art images without any pre-existing labels or masks*. To tackle this problem, we divide each line art image into a set of patches and propose a Transformer-based framework that learns patch-level similarities within and across images. We then apply edge-aware clustering and a region matching algorithm to convert patch-level predictions into coherent region-level correspondences. To support training and evaluation, we develop an automatic annotation pipeline and manually refine a subset of the data to construct benchmark datasets. Experiments on multiple datasets demonstrate that our method achieves high patch-level accuracy (e.g., 96.34%) and generates consistent region-level correspondences, highlighting its potential for real-world manga applications.

## Introduction

In traditional manga and animation production, artists often need to manually identify and annotate semantic regions across various line art frames to maintain consistency in coloring and character appearance. This process is labor-intensive and requires a high level of precision and artistic skill. To address this issue, we explore the fundamental problem of understanding structural regions in a line art image and predicting region-wise correspondences between different line art images, as shown in Figure 1.

However, predicting region-wise correspondence in line art is particularly challenging. Unlike natural images, line art images are abstract and sparse, lacking texture and color cues that usually guide visual matching. Characters may appear in different poses, scales, or viewpoints, and the level of abstraction may vary depending on the artist’s style. These variations make it difficult to determine which regions are

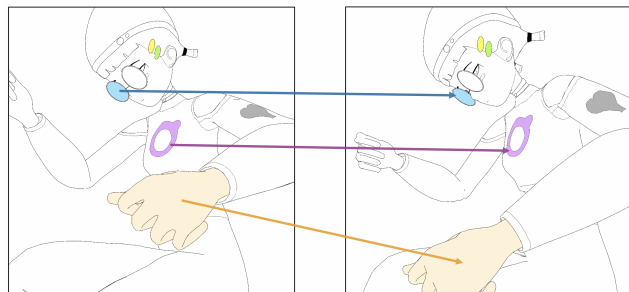


Figure 1: Given a pair of manga line art images, our task is to match the corresponding regions across the two images. Regions with the same color represent corresponding parts between the two images.

semantically related. A more fundamental technical limitation arises from the lack of datasets with region-level segmentation annotations for line art. As a result, existing segmentation methods are mostly trained on natural images. However, regions in line art images are defined by hand-drawn contours, which are often open or loosely formed, making them fundamentally different from the closed, well-separated regions in natural images. This domain gap significantly limits the effectiveness of existing methods in producing accurate and fine-grained segmentation for line art. Due to both the abstract nature of line art and the lack of effective segmentation methods for such images, region-wise correspondence prediction remains largely underexplored.

Previous works on correspondence prediction in line art often rely on the assumption that line art images have already been segmented into closed regions (Dai et al. 2024). However, this assumption does not hold in practical scenarios. In this paper, we explore a new task: *predicting region-wise correspondence directly from raw line art without any prior segmentation or annotations*. Given a pair of unannotated line art images, our goal is to divide each image into semantically meaningful regions and predict the correspondences between them.

Considering the abstract nature of line art and the challenges of this task, we propose a Transformer-based pipeline that jointly learns intra-image and cross-image features. Specifically, we divide each raw manga line art image into

\*This work was conducted when the first author was a research intern at CyberAgent, Inc.

†Corresponding Author

a set of patches and extract their features using a composite Transformer model, which learns to capture patch-level similarities. We then merge adjacent patches with high intra-image similarity to obtain initial region groups. Since the boundaries of these patch clusters are inherently blocky, we further introduce an edge-aware post-processing step to refine them into pixel-level regions with smooth, stroke-aligned boundaries, effectively overcoming the technical bottleneck of line art segmentation. Finally, we aggregate the cross-image patch similarities to derive region-wise correspondence predictions between line art images.

To support training in the absence of human annotations, we build an automatic pipeline that performs pixel-level segmentation and correspondence matching, generating a large-scale pseudo-labeled dataset. For evaluation, we manually refine a subset of these pseudo labels to construct a high-quality benchmark dataset. We evaluate our approach on multiple manga line art datasets, including both synthetic and real-world examples. Experimental results demonstrate that our method accurately predicts patch-level similarities and produces coherent region-level correspondences across images.

To summarize, our contributions are as follows:

- We are the first to study region-wise correspondence prediction between raw manga line art images, contributing to a deeper structural understanding of line art images.
- We propose a Transformer-based framework that learns patch-level similarities and enables coherent region-level correspondences, demonstrating its effectiveness across diverse line art datasets.
- We develop an automatic annotation pipeline and construct a manually refined benchmark dataset with region-level ground-truth correspondences to support quantitative evaluation.

## Related Work

### Manga Line Art Datasets

Manga line art datasets can be broadly classified based on how the line art is obtained, which significantly affects the structural complexity and realism of the resulting data.

One common method involves extracting contour lines from 3D-rendered characters. This pipeline produces clean, closed-contour line art with well-defined semantic parts, making it easier to segment and annotate. Notable examples include AnimeRun (Siyao et al. 2022) and PaintBucket-Character (PBC) (Dai et al. 2024). The PBC dataset, in particular, provides over 10,000 synthetic line art images paired with part-level semantic labels across consistent character poses and viewpoints. We use PBC as one of the datasets for training and evaluation.

In contrast, a more realistic but challenging approach is to extract line art from real-world anime frames. These frames are processed using learned line detection models such as LineArtDetector (Zhang, Rao, and Agrawala 2023) used in MangaNinja (Liu et al. 2025). The resulting line art better reflects the characteristics of hand-drawn manga: open contours, abstract shapes, and diverse drawing styles. Among

such datasets of real-world anime frames, ATD-12K (Siyao et al. 2021) is a representative example, containing 12,000 high-quality keyframe pairs from professional anime. We convert these frames to line art and evaluate our method under these more complex and less structured conditions. To further test generalization, we additionally generate line art pairs from text-to-image synthesis models.

### Matching in Line Art

Recent studies in line art processing have explored point-to-point matching to enhance tasks like automatic colorization (Meng et al. 2025; Liu et al. 2025). These methods rely on techniques from natural image matching (Lindenberger, Sarlin, and Pollefeys 2023), which use visual cues like color and texture. However, such cues are absent in line art, leading to sparse and unreliable keypoints.

On the other hand, some works have explored region-wise matching (Dai et al. 2024), but they typically assume that regions are pre-segmented or enclosed by clean, closed contours. In such settings, regions can be effectively extracted via rule-based methods, but this setup does not apply to raw, hand-drawn line art.

In contrast to prior work, our approach tackles region-wise correspondence prediction directly from unannotated line art. Our method generates pseudo-labels through automatic region segmentation and matching, enabling supervised training of a Transformer model. This provides a new solution for understanding structure in raw manga line art.

## Approach

In this section, we introduce our proposed framework, which consists of two main components: **a Transformer-based model for patch-level similarity learning**, and **a post-processing method to predict region-wise correspondences**. Figure 2 illustrates how our method takes a raw pair of manga line art images as input and produces region-wise correspondence predictions.

Given an unannotated pair of line art images  $I_a$  and  $I_b$ , we first divide each image into  $N$  patches of size  $p \times p$ , denoted as  $P_a, P_b \in \mathbb{R}^{N \times p \times p}$ . These patches are embedded and processed by a Vision Transformer  $f_{\text{ViT}}$  to extract patch-level features. We then use a Multiplex Transformer to model intra-image structures and cross-image relationships, and compute a dense patch similarity matrix  $S \in [0, 1]^{2N \times 2N}$ . Finally, we apply a post-processing step that first clusters similar patches into region groups  $\mathcal{R}_a$  and  $\mathcal{R}_b$  based on the intra-image similarities in  $S$ , and then predicts region-level correspondences  $\mathcal{M} \subseteq \mathcal{R}_a \times \mathcal{R}_b$  based on the cross-image similarities in  $S$ .

In the following sections, we describe each component of our pipeline in detail.

### Patch-Level Similarity Learning

**Feature Extraction.** Different from conventional matching approaches (e.g., point-to-point matching) that often rely on CNN-based feature extractors (Sun et al. 2021; Wang et al. 2024), we adopt a Vision Transformer (ViT) (Dosovitskiy et al. 2020) to learn patch-level features, which are better

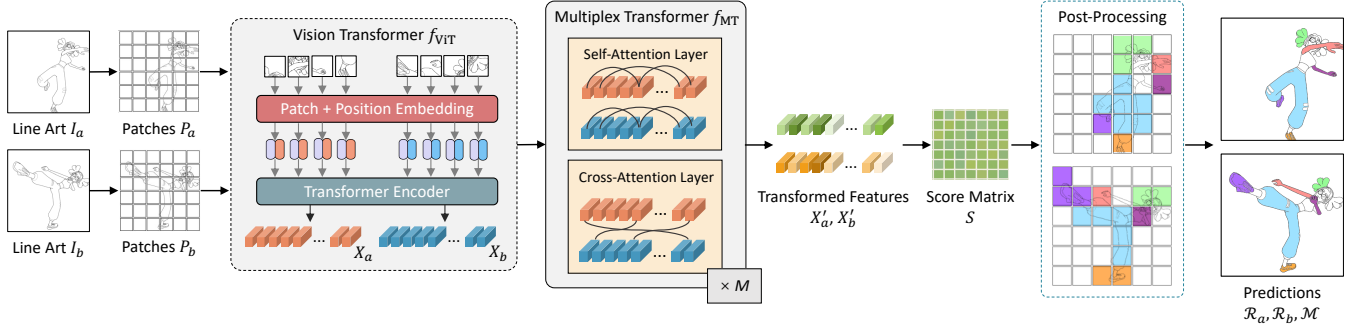


Figure 2: Overview of our proposed pipeline for predicting region-wise correspondence between manga line art images. The model extracts patch-level features using a Vision Transformer and predicts patch-level similarity via a Multiplex Transformer, followed by post-processing to obtain region-level correspondence.

suited for capturing region-level semantic structures in line art images.

Given patch sets  $P_a$  and  $P_b$  extracted from the two images, we first map each patch into a  $d$ -dimensional token via a linear embedding layer, yielding  $Z_a, Z_b \in \mathbb{R}^{N \times d}$ . We then add learnable positional embeddings  $E_{\text{pos}} \in \mathbb{R}^{N \times d}$  to encode spatial layout:

$$\tilde{X}_a = Z_a + E_{\text{pos}}, \quad \tilde{X}_b = Z_b + E_{\text{pos}}. \quad (1)$$

The Vision Transformer encoder processes the resulting sequences through multiple stacked self-attention layers to produce patch-level feature representations:

$$X_a = f_{\text{ViT}}(\tilde{X}_a), \quad X_b = f_{\text{ViT}}(\tilde{X}_b), \quad (2)$$

where  $X_a, X_b \in \mathbb{R}^{N \times d}$  denote the final token features of images  $I_a$  and  $I_b$ .

**Multiplex Transformer.** We feed the extracted features  $X_a, X_b$  into the Multiplex Transformer  $f_{\text{MT}}$ , which consists of  $M$  stacked layers, each containing both self-attention and cross-attention blocks (Vaswani et al. 2017). At each layer, tokens from both  $X_a$  and  $X_b$  perform self-attention and attend to tokens in the other image via cross-attention. This design enables the model to capture both intra-image structure and cross-image correspondence simultaneously.

After  $M$  blocks, we obtain the transformed patch features  $X'_a, X'_b \in \mathbb{R}^{N \times d}$ :

$$X'_a, X'_b = f_{\text{MT}}(X_a, X_b). \quad (3)$$

These transformed features are used in the next stage to compute patch-wise similarity across the two images.

**Similarity Computation.** Given the transformed patch features  $X'_a, X'_b$ , we compute a unified similarity matrix  $S \in [0, 1]^{2N \times 2N}$ , which contains both intra-image and cross-image similarities, using cosine similarity followed by row-wise softmax. The matrix  $S$  encodes intra-image similarity (within  $I_a$  and  $I_b$ ) as well as cross-image similarity (between  $I_a$  and  $I_b$ ) in a unified structure.

**Ground-Truth Matrix.** We construct the ground-truth patch correspondence matrix  $G \in \{0, 1\}^{2N \times 2N}$  as follows. After dividing each image into  $N$  patches, we assign a region ID to

each patch by selecting the most frequent region label within the patch, provided it occupies more than 55% of the patch area. Two patches within the same image are considered to belong to the same region if they share the same region ID. For cross-image correspondences, we mark entries in  $G$  as 1 for all patch pairs whose underlying regions are annotated as corresponding across the two images ( $I_a$  and  $I_b$ ).

**Loss Function.** Since the ground-truth matrix  $G$  is highly sparse, naively supervising all  $2N \times 2N$  pairs makes training hard to converge and limits performance. To cope with this, we adopt a CLIP-style sampled contrastive loss (Radford et al. 2021). During training, we randomly draw a subset of positive pairs from the nonzero entries of  $G$ . For each sampled positive  $(i, j)$ , we choose  $K$  negatives  $\{j_k\}_{k=1}^K$  that are not matched with  $i$ . We then compute a temperature-scaled softmax over  $\{j\} \cup \{j_k\}_{k=1}^K$  in the  $i$ -th row of  $S$  and minimize the negative log-likelihood:

$$\mathcal{L}_{i,j} = -\log \frac{\exp(S_{ij}/\tau)}{\exp(S_{ij}/\tau) + \sum_{k=1}^K \exp(S_{ij_k}/\tau)}, \quad (4)$$

where  $\tau$  is a temperature parameter. The final loss is averaged over all sampled positives in the batch, enabling the model to learn meaningful patch-level similarities under sparse supervision.

## Region Matching via Post-Processing

**Intra-Image Patch Merging.** To derive region-level correspondences from the patch-level similarity matrix produced by our Transformer-based model, we first perform intra-image patch merging as a post-processing step.

As illustrated in Figure 3, for image  $I_a$ , we extract the intra-image similarity submatrix  $S_{aa} \in [0, 1]^{N \times N}$  from the upper-left block of the full similarity matrix  $S$ , which represents pairwise similarities among all patches within  $I_a$  (similarly,  $S_{bb}$  is used for  $I_b$ ). We compute a structural edge map  $E_a$  from  $I_a$  by applying Gaussian smoothing followed by Sobel gradients (Sobel, Feldman et al. 1968). Adjacent patches within an 8-neighborhood are merged based on their similarity in  $S_{aa}$ , while merges across strong edges are suppressed by checking the average edge response along shared

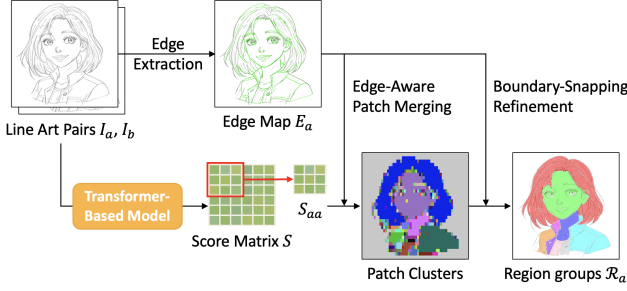


Figure 3: Framework of intra-image patch merging. From a structural edge map extracted from the line art and patch clusters derived from patch-level predictions, our edge-aware merging and watershed refinement yield a set of edge-constrained pixel-wise region groups.

boundaries. We then apply a watershed algorithm on  $E_a$  using the merged patch clusters as seeds, so that the resulting region boundaries align with the stroke structure. To avoid fragmented segmentation, we further merge small regions based on contact length and edge strength in an edge-aware manner. Finally, each patch is assigned a region ID via majority voting over its pixels, producing the final pixel-wise region map  $\mathcal{R}_a$ .

**Cross-Image Region Matching.** Given the region sets  $\mathcal{R}_a$  and  $\mathcal{R}_b$ , we derive region-level similarities by aggregating the cross-image patch similarity submatrices  $S_{ab}, S_{ba} \in [0, 1]^{N \times N}$ . Here,  $S_{ab}$  corresponds to the upper-right block of the full similarity matrix  $S$  and encodes patch-wise similarities from image  $I_a$  to image  $I_b$ , while  $S_{ba}$  corresponds to the lower-left block and encodes similarities in the reverse direction.

For each region pair  $(R_i, R_j)$  with  $R_i \in \mathcal{R}_a$  and  $R_j \in \mathcal{R}_b$ , we compute the directional similarity from  $R_i$  to  $R_j$  as:

$$s(R_i, R_j) = \frac{1}{|R_i| |R_j|} \sum_{p \in R_i} \sum_{q \in R_j} S_{ab}[p, q], \quad (5)$$

where  $S_{ab}[p, q]$  denotes the similarity from patch  $p$  in  $I_a$  to patch  $q$  in  $I_b$ . Note that the similarity is asymmetric:  $s(R_i, R_j)$  is computed from  $S_{ab}$ , while  $s(R_j, R_i)$  is computed from  $S_{ba}$ .

To determine region-level correspondences, we perform threshold-based greedy matching in both directions. Specifically, for each region in  $\mathcal{R}_a$ , we select all regions in  $\mathcal{R}_b$  whose similarity  $s(R_i, R_j)$  exceeds a predefined threshold, resulting in the forward match set  $\mathcal{M}_{a \rightarrow b}$ . Likewise, we compute the reverse matches  $\mathcal{M}_{b \rightarrow a}$  using  $S_{ba}$ . The final correspondence set is defined as the union  $\mathcal{M} = \mathcal{M}_{a \rightarrow b} \cup \mathcal{M}_{b \rightarrow a}$ .

## Annotation Dataset Construction

To support both training and evaluation of the proposed framework, we require datasets containing region-wise correspondences between pairs of manga line art images. Since no existing dataset provides such annotations, we construct the necessary data through two separate approaches.

For training, we develop an automatic annotation pipeline that generates large-scale supervision using colored line art as auxiliary input. This process consists of two main stages: (1) segmenting each line art image into coherent regions based on color guidance; (2) establishing region-level correspondences between paired line art images using appearance and spatial cues.

For evaluation, however, high-quality ground truth is essential. Therefore, we manually annotate a subset of image pairs with accurate region segmentation and correspondence labels. This manually curated dataset enables reliable benchmarking of our model’s performance under realistic and challenging conditions.

## Automatically Annotated Training Datasets

**Automatic Intra-Image Segmentation.** Most existing deep learning-based segmentation methods are trained on natural images, as region-segmented datasets for manga line art are scarce. However, the domain gap between natural images and line art causes these models to struggle with fine-grained segmentation on line art images. To address this issue, we adopt a rule-based method that leverages the inherent color structure of colored line art. We segment colored line art by clustering pixels into  $K$  dominant colors, detecting connected regions via color similarity, and merging small fragments based on both color and boundary cues.

**Automatic Cross-Image Matching.** After obtaining the region segmentation masks, we construct region-wise correspondences between line art pairs. We first perform point-to-point matching using LightGlue (Lindemberger, Sarlin, and Pollefeys 2023). Since the extracted keypoints are often concentrated near structural boundaries and are relatively sparse on line art images, we expand each keypoint to a  $5 \times 5$  pixel neighborhood to increase coverage and improve robustness in subsequent region matching. For each region in image  $I_a$ , we filter the matched keypoints by comparing the color of each keypoint’s pixel to the average color of the region. Points with large deviations are discarded. We then count the occurrences of target regions in  $I_b$  where the remaining keypoints are matched, and assign the region in  $I_b$  with the highest vote count as the corresponding match of the region in  $I_a$ .

Additionally, since point-to-point keypoints tend to be overly concentrated on facial areas of characters, we further apply a coarse matching step for unmatched regions. We adopt a rule-based matching method that considers both positional alignment and color similarity between regions.

## Manually Refined Evaluation Datasets

While our training pipeline relies on automatically generated region segmentation and correspondences, accurate evaluation requires ground-truth annotations that reflect human-level understanding of semantic regions and their matches. To address this need, we construct manually refined evaluation datasets, covering both synthetic and real-world manga line art. These datasets serve as standard benchmarks for assessing model performance.

As illustrated in Figure 4, we compare the automatically generated region correspondences with the manually cor-



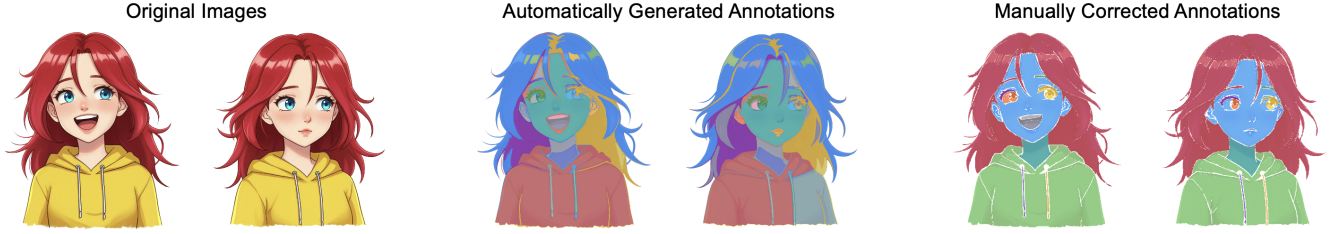


Figure 4: An example of automatic region matching results and manually corrected ground truth. Regions with the same color across the two images indicate a matched region pair, while gray denotes regions without a match.

rected ground truth. These comparisons demonstrate that our automatic annotation pipeline provides reasonable supervision for training, while also highlighting the necessity of manual refinement for reliable evaluation.

We will release the full annotation pipeline, manual correction tools, and the evaluation dataset to facilitate future research.

## Experiments

### Datasets for Training and Evaluation

As discussed in the section of Related Work, we conduct experiments on two types of manga line art datasets, differing in how the line art is obtained and their level of structural complexity.

**3D-Rendered Line Art.** We use the PaintBucket-Character (PBC) (Dai et al. 2024) dataset for both training and evaluation. We sample pairs of frames separated by seven frames within the same animation sequence, defining region correspondences based on shared part-level semantic labels. For example, region 19 in the left image of Figure 5 and region 40 in the right image share label ID 23, indicating a semantic match.

In our experiments, we randomly sample 300 image pairs (595 images) for testing, and use the remaining 10,961 pairs (11,336 images) for training.

**Hand-Drawn Manga Style Line Art.** For training on hand-drawn style data, we use an in-house dataset constructed from short anime clips. Frame pairs are sampled every 18 frames, converted to line art using the MangaNinja method (Liu et al. 2025), and annotated using our automatic pipeline, yielding 20,000 (39,602 images) image pairs.

For evaluation, we use the ATD-12K (ATD) (Siyao et al. 2021) dataset and a synthetic dataset (GenAI) generated via the Imagen diffusion model (Saharia et al. 2022). For both datasets, we extract line art using the same method and manually refine region correspondences – 25 pairs (50 images) for ATD and 20 pairs (40 images) for GenAI. An example of the annotated data is shown in Figure 4.

### Implementation Details

We adopt a ViT-B/16 backbone pre-trained on ImageNet (Dosovitskiy et al. 2020), and normalize the input images using the standard ImageNet mean and standard deviation to match the requirements of the pre-trained model. To fully leverage the capacity of ViT, we use its default

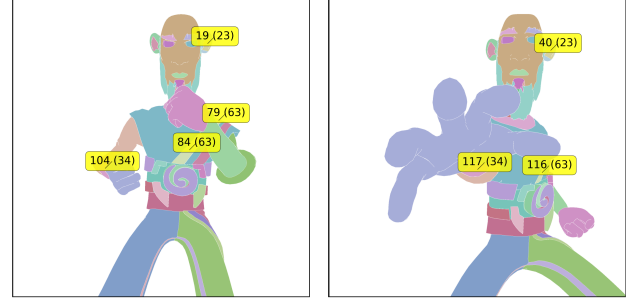


Figure 5: Example of region-level correspondence annotations in the PBC dataset. Matched regions are visualized using the same color across two images. Yellow boxes display the region ID and label ID of each region in the format Region ID (Label ID).

patch size of  $16 \times 16$ . Our Multiplex Transformer consists of  $M = 4$  stacked layers of self-attention and cross-attention. The model is trained for 20 epochs with a batch size of 16, using the AdamW optimizer and an initial learning rate of  $1 \times 10^{-4}$ . A learning rate scheduler combining a warm-up phase with cosine annealing is applied. The whole process is conducted on a single NVIDIA A100 GPU.

### Quantitative Results

**Patch-Level Evaluation.** We first assess how well our Transformer-based model captures patch-level semantic similarities by comparing the predicted similarity matrix  $S$  against the ground-truth correspondence matrix  $G$ . We conduct experiments on three datasets: PBC, ATD, and GenAI, and report the results in Table 1.

We evaluate both intra-image similarity (within the same image) and cross-image similarity (between image pairs) using the following metrics. First, we compute precision-recall (PR) curves (Figure 6) by thresholding similarity scores and report standard metrics including Average Precision (AP), best F1 score, and the corresponding precision and recall at the optimal threshold. For cross-image evaluation, we also report top- $K$  accuracy, defined as the percentage of ground-truth matched patches whose true match appears among the top- $K$  most similar patches in the other image.

As shown in Table 1 and Figure 6, our model achieves near-perfect intra-image performance on the PBC dataset,

Datasets	Matching Type	AP	Best F1	Precision	Recall	Top-1 Accuracy	Top-5 Accuracy
PBC	Intra-img ( $I_a$ )	99.92	98.57	99.06	98.08	—	—
	Intra-img ( $I_b$ )	99.93	98.66	98.92	98.40	—	—
	Cross-img	98.86	95.23	96.34	94.15	85.44	91.35
ATD	Intra-img ( $I_a$ )	85.40	76.79	78.16	75.46	—	—
	Intra-img ( $I_b$ )	82.11	73.18	69.70	77.03	—	—
	Cross-img	80.53	71.71	69.10	74.53	83.59	92.17
GenAI	Intra-img ( $I_a$ )	84.52	76.28	74.89	77.73	—	—
	Intra-img ( $I_b$ )	86.22	77.34	74.36	80.57	—	—
	Cross-img	84.48	75.52	72.23	79.14	75.94	85.74

Table 1: Patch-level evaluation on PBC, ATD, and GenAI datasets (percentage values).

Dataset	Matching Type	ARI	mIoU (P→G)	mIoU (G→P)	CR	Region Precision	Region Recall
PBC	Intra-img ( $I_a$ )	83.05	60.20	20.30	0.32	—	—
	Intra-img ( $I_b$ )	83.86	60.34	19.97	0.32	—	—
	Cross-img	—	—	—	—	59.92	21.37
ATD	Intra-img ( $I_a$ )	55.11	32.37	37.88	1.37	—	—
	Intra-img ( $I_b$ )	50.37	29.74	35.90	1.49	—	—
	Cross-img	—	—	—	—	72.41	32.93
GenAI	Intra-img ( $I_a$ )	46.82	37.07	31.59	1.04	—	—
	Intra-img ( $I_b$ )	56.81	40.35	36.38	1.07	—	—
	Cross-img	—	—	—	—	68.52	22.05

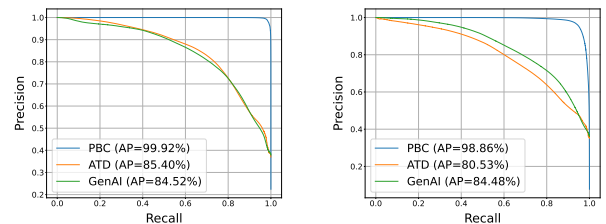
Table 2: Region-level evaluation on PBC, ATD, and GenAI datasets (percentage values; CR is shown in raw value). Region Precision and Region Recall are computed using predicted region pairs with purity  $> 0.8$ .

with AP scores above 99.9% and best F1 scores over 98.5% for both  $I_a$  and  $I_b$ . This indicates that the model effectively captures internal region consistency in well-structured synthetic line art. On the more challenging ATD and GenAI datasets—designed to simulate real-world line art—intra-image AP remains above 82%, and best F1 scores exceed 73%, demonstrating the model’s strong generalization.

In the cross-image setting, our model achieves a level of performance comparable to the intra-image case, confirming its ability to learn patch-level correspondences across image pairs. This robustness is largely attributed to our Transformer’s joint learning of intra-image and cross-image features, which enables effective matching even in the absence of color and texture cues.

**Region-Level Evaluation.** We further evaluate our method at the region level, focusing on two aspects: (1) *intra-image region grouping via patch merging*, and (2) *cross-image region correspondence prediction*. Results on the PBC, ATD, and GenAI datasets are shown in Table 2.

To assess the quality of patch clustering within each image, we compare the predicted region groups  $\mathcal{R}_a$  and  $\mathcal{R}_b$  with the pixel-level ground-truth segmentation using three metrics: Adjusted Rand Index (ARI), mean Intersection over Union from prediction to ground truth (mIoU P→G), and from ground truth to prediction (mIoU G→P). We also report the Cluster Ratio (CR), which measures the average number of predicted regions per ground-truth region.



(a) Intra-image ( $I_a$ ) Matching (b) Cross-image Matching

Figure 6: Precision-recall (PR) curves for intra-image and cross-image patch-level matching.

Ideally, CR should be close to 1, indicating a balanced segmentation. A CR much lower than 1 suggests under-segmentation (i.e., multiple ground-truth regions are merged into one), while a CR significantly higher than 1 implies over-segmentation, where individual regions are unnecessarily fragmented. For cross-image evaluation, we adopt a strategy inspired by visual relationship detection (Xu et al. 2017). Specifically, we compute region-wise precision and recall based on region pairs whose predicted correspondences have a purity score greater than 0.8. This ensures that only meaningful and consistent matches are considered.

As shown in Table 2, our post-processing pipeline per-

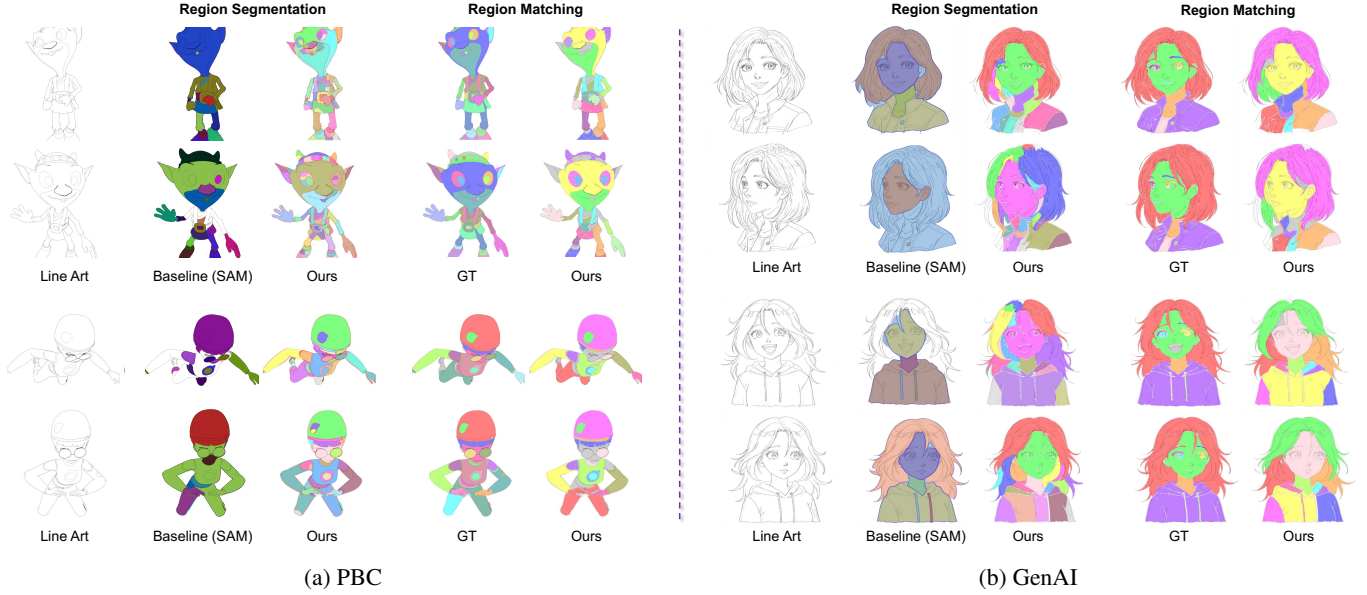


Figure 7: Visualization examples on the PBC and GenAI datasets. In the region segmentation results, the same color within an image denotes a single region, and white indicates the background. In the region matching results, the same color across two images indicates a matched region pair, while gray denotes regions without a match.

forms well on the PBC dataset, which features clean, closed contours and fewer regions per image. Specifically, we achieve an ARI exceeding 83% and an mIoU (P→G) of approximately 60%, indicating robust intra-image clustering performance. In contrast, performance on ATD and GenAI is lower, reflecting the challenges posed by real-world or realistically styled line art. In terms of cross-image region matching, our method achieves reasonable region precision, demonstrating its ability to identify meaningful correspondences. However, region recall remains relatively low (20-30%), suggesting that our method struggles with matching small fragmented regions or large semantic regions that are inconsistently segmented (e.g., hair or clothing divided into multiple parts). This highlights the difficulty of consistent region matching in highly abstract line art.

## Qualitative Results

We qualitatively evaluate our method on multiple datasets, with examples shown in Figure 7. As in our quantitative evaluation, we analyze the results from two aspects: (1) *intra-image region segmentation* and (2) *cross-image region matching*.

For region segmentation, we compare our method with the Segment Anything Model (SAM) (Kirillov et al. 2023), a strong baseline for natural images. As shown in Figure 7, SAM often merges distinct semantic parts (e.g., hair or clothing) with the background and fails to produce fine-grained boundaries due to the lack of color, texture, and shading cues. In contrast, our method generates more precise and semantically coherent regions.

For region matching, our approach accurately aligns major regions, including challenging PBC scenes with large pose changes and significant shape deformation. Our region

correspondence results demonstrate promising performance and align well with human perception in many cases. This is inherently challenging and has received limited prior attention, with no established baselines for direct comparison. To our knowledge, our method is the first to enable such correspondence for manga line art.

## Limitation

Nevertheless, there is still a gap compared with manually annotated ground truth for cross-image region matching. For instance, to avoid over-segmentation, we merge small regions during post-processing. This can lead to the loss of fine-grained semantic details – such as eyes and eyebrows being merged into larger facial regions. We acknowledge this trade-off as a current limitation and plan to address it through improvements to both the model architecture and the post-processing pipeline. Additionally, we aim to extend our approach to handle more diverse manga styles and complex scenes, improve its robustness in real-world scenarios, and explore its integration into downstream applications.

## Conclusion

In this paper, we explored a realistic and previously underexplored task: predicting region-wise correspondence between manga line art images without any prior segmentation or annotations. We proposed a Transformer-based framework that jointly learns intra-image and cross-image features from raw line art images, and introduced a post-processing method that aggregates and refines the patch-level predictions into region-level correspondences. To support training and evaluation, we developed an automatic annotation pipeline and manually refined a subset of the annotations to construct

benchmark evaluation datasets. Experiments on multiple datasets demonstrate that our model achieves high patch-level accuracy and produces coherent region-level correspondences. In future work, we plan to apply our region correspondence model to downstream tasks such as automatic line art colorization and frame interpolation, where consistent region-wise understanding plays a critical role.

## References

- Dai, Y.; Zhou, S.; Li, Q.; Li, C.; and Loy, C. C. 2024. Learning inclusion matching for animation paint bucket colorization. In *Proceedings of the IEEE/CVF Conference on Computer Vision and Pattern Recognition*, 25544–25553.
- Dosovitskiy, A.; Beyer, L.; Kolesnikov, A.; Weissenborn, D.; Zhai, X.; Unterthiner, T.; Dehghani, M.; Minderer, M.; Heigold, G.; Gelly, S.; et al. 2020. An Image is Worth 16x16 Words: Transformers for Image Recognition at Scale. In *Proceedings of the International Conference on Learning Representations*.
- Kirillov, A.; Mintun, E.; Ravi, N.; Mao, H.; Rolland, C.; Gustafson, L.; Xiao, T.; Whitehead, S.; Berg, A. C.; Lo, W.-Y.; et al. 2023. Segment anything. In *Proceedings of the IEEE/CVF International Conference on Computer Vision*, 4015–4026.
- Lindenberger, P.; Sarlin, P.-E.; and Pollefeys, M. 2023. LightGlue: Local Feature Matching at Light Speed. In *Proceedings of the IEEE/CVF International Conference on Computer Vision*, 17627–17638.
- Liu, Z.; Cheng, K. L.; Chen, X.; Xiao, J.; Ouyang, H.; Zhu, K.; Liu, Y.; Shen, Y.; Chen, Q.; and Luo, P. 2025. Manganinja: Line art colorization with precise reference following. In *Proceedings of the Computer Vision and Pattern Recognition Conference*, 5666–5677.
- Meng, Y.; Ouyang, H.; Wang, H.; Wang, Q.; Wang, W.; Cheng, K. L.; Liu, Z.; Shen, Y.; and Qu, H. 2025. Anidoc: Animation creation made easier. In *Proceedings of the IEEE/CVF Computer Vision and Pattern Recognition Conference*, 18187–18197.
- Radford, A.; Kim, J. W.; Hallacy, C.; Ramesh, A.; Goh, G.; Agarwal, S.; Sastry, G.; Askell, A.; Mishkin, P.; Clark, J.; et al. 2021. Learning transferable visual models from natural language supervision. In *Proceedings of the International Conference on Machine Learning*, 8748–8763. PmLR.
- Saharia, C.; Chan, W.; Saxena, S.; Li, L.; Whang, J.; Denton, E. L.; Ghasemipour, K.; Gontijo Lopes, R.; Karagol Ayan, B.; Salimans, T.; et al. 2022. Photorealistic text-to-image diffusion models with deep language understanding. *Advances in Neural Information Processing Systems*, 35: 36479–36494.
- Siyao, L.; Li, Y.; Li, B.; Dong, C.; Liu, Z.; and Loy, C. C. 2022. Animerun: 2d animation visual correspondence from open source 3d movies. *Advances in Neural Information Processing Systems*, 35: 18996–19007.
- Siyao, L.; Zhao, S.; Yu, W.; Sun, W.; Metaxas, D.; Loy, C. C.; and Liu, Z. 2021. Deep animation video interpolation in the wild. In *Proceedings of the IEEE/CVF Conference on Computer Vision and Pattern Recognition*, 6587–6595.
- Sobel, I.; Feldman, G.; et al. 1968. A 3x3 isotropic gradient operator for image processing. *a talk at the Stanford Artificial Project in*, 1968: 271–272.
- Sun, J.; Shen, Z.; Wang, Y.; Bao, H.; and Zhou, X. 2021. LoFTR: Detector-free local feature matching with transformers. In *Proceedings of the IEEE/CVF Computer Vision and Pattern Recognition Conference*, 8922–8931.
- Vaswani, A.; Shazeer, N.; Parmar, N.; Uszkoreit, J.; Jones, L.; Gomez, A. N.; Kaiser, Ł.; and Polosukhin, I. 2017. Attention is all you need. *Advances in Neural Information Processing Systems*, 6000–6010.
- Wang, Y.; He, X.; Peng, S.; Tan, D.; and Zhou, X. 2024. Efficient LoFTR: Semi-dense local feature matching with sparse-like speed. In *Proceedings of the IEEE/CVF Computer Vision and Pattern Recognition Conference*, 21666–21675.
- Xu, D.; Zhu, Y.; Choy, C. B.; and Fei-Fei, L. 2017. Scene graph generation by iterative message passing. In *Proceedings of the IEEE Conference on Computer Vision and Pattern Recognition*, 5410–5419.
- Zhang, L.; Rao, A.; and Agrawala, M. 2023. Adding conditional control to text-to-image diffusion models. In *Proceedings of the IEEE/CVF International Conference on Computer Vision*, 3836–3847.